Journal of Tropical Forest Science 37(Special Issue): 112–120 (2025)
https://doi.org/10.26525/jtfs2025.37S.SI.112
ISSN: 0128-1283, eISSN: 2521-984

CHARACTERISATION AND IDENTIFICATION OF *KAEMPFERIA PARVIFLORA*, *CURCUMA CAESIA* AND *CURCUMA AERUGINOSA* BY MULTI-STEPS INFRARED SPECTROSCOPY AND CHEMOMETRIC ANALYSIS

Fauziah A[1,] *, Tan AL[2], Salbiah M[1], Ummu Hani B[2], Nur Munirah S[2] & Hani Idayu B[2]

[1] *Herbal Quality Control Programme, Natural Products Division, Forest Research Institute Malaysia, 52109 Kepong, Selangor*
[2] *Biological Resources Programme, Natural Products Division, Forest Research Institute Malaysia, 52109 Kepong, Selangor*

**fauziahabdullah@frim.gov.my*

Submitted June 2024; accepted December 2024

Kaempferia parviflora, *Curcuma caesia*, and *Curcuma aeruginosa*, belonging to the Zingiberaceae family (Tribe Hedychieae), have not only been utilised for medicinal purposes in Malaysia, but also in traditional Chinese and Ayurvedic medicine. They share great similarities in morphology and external appearance with certain genera; hence, their identification is sometimes difficult. In addition, the raw materials that are distributed or sold are usually pulverised into small pieces, which hinders morphological identification. Herbal suppliers, manufacturers, and consumers often encounter confusion when purchasing rhizomes using vernacular names such as kunyit hitam, temu ireng, and temu hitam, which can be used interchangeably among the three species. The controversial taxonomy of these species of the tribe Hedychieae further complicates their correct identification, which is crucial for ensuring their pharmacological and clinical efficacy. In this study, we employed a multi-step infrared (IR) spectroscopy method combined with a chemometrics approach to distinguish these closely related species. We analysed 53 samples (19 *K. parviflora*, 17 *C. caesia*, and 17 *C. aeruginosa*) collected from 23 locations across Peninsular Malaysia. The species were effectively differentiated using one-dimensional IR (1D-IR), second derivative IR, and two-dimensional correlation infrared (2D-IR) spectra. Principal component analysis (PCA) of the 1D-IR spectra further confirmed the clear separation of the three species. Our findings demonstrate that macroscopic IR spectroscopy, when paired with chemometrics, is a useful and nondestructive approach for the initial quality control and identification of herbal raw materials.

Keywords: *K. parviflora, C. caesia, C. aeruginosa*, multi-steps infrared spectroscopy, chemometrics analysis

INTRODUCTION

Members of the Zingiberaceae family are renowned for their medicinal uses in Malaysia, traditional Chinese medicine, and Ayurvedic practices. Identifying these species solely by morphology, especially without their inflorescences, presents challenges due to their similar appearance. Studies have highlighted the difficulty in genus-level identification for Zingiberaceae species native to Peninsular Malaysia (Leong–Skornickova et al. 2010, Ibrahim et al. 2007). The demand for herbal products derived from Zingiberaceae, particularly from the Hedychieae tribe, has surged recently, with species like *Curcuma aeruginosa* (temu ireng), *Curcuma caesia* (temu hitam), and *Kaempferia parviflora* (kunyit hitam) being openly traded in various forms including fresh or dried slices. These species have a long history of cultivation in Peninsular Malaysia, primarily for medicinal and culinary purposes (Ridley 1924). *C. aeruginosa* is traditionally used to treat sores (Nik Musa'adah et al. 2017a), while *C. caesia* finds application in fracture treatment, acne relief, and nerve pain alleviation, with the leaves also used in postnatal bathing (Nik Musa'adah et al. 2017b). *K. parviflora*, on the other hand, has been utilized in Thailand for its anti-inflammatory properties, aiding in wound healing, diarrhea, and colic management (Than et al. 2019).

Among the three species, *K. parviflora* is distinguishable by its smaller, herbaceous stature and broad ovate leaves, while *C. aeruginosa* and *C. caesia* are medium-

sized with oblong to lanceolate leaves. The bladeless leaf sheath of *C. aeruginosa* is green, contrasting with the reddish brown of *C. caesia*. Rhizome identification is also challenging due to environmental and age variations, with each species presenting distinct inner rhizome colours and scents. Routine morphological identification is often impractical for manufacturers who frequently deal with preprocessed raw materials. Given the morphological similarities and the variations caused by environmental factors, a more reliable method is required for accurate species identification. Chemical analysis offers a viable solution, providing precise differentiation based on the unique chemical profiles of each species. Methods such as High-Performance Liquid Chromatography (HPLC) and High-Performance Thin-Layer Chromatography (HPTLC) are efficient but not cost-effective and require extensive sample preparation prior to analysis.

In contrast, Fourier-transform infrared (FT-IR) spectroscopy offers several advantages. For accurate species, identification of *K. parviflora, C. caesia*, and *C. aeruginosa*, Fourier-transform infrared (FT-IR) spectroscopy combined with principal component analysis (PCA) offers a promising solution. This method is cost-effective, rapid, and requires minimal sample preparation, making it suitable for routine quality control and high-throughput screening of herbal raw materials. FT-IR spectroscopy is effective in distinguishing between different herbal species by analyzing their unique chemical profiles. The technique measures the absorption of infrared radiation, producing a spectrum that represents the molecular fingerprint of a sample. This spectrum can be used to identify key functional groups and chemical bonds present in the material (Tew et al. 2022, Pramod et al. 2011). The integration of chemometric methods like PCA further enhances the discrimination power of FT-IR spectroscopy. PCA simplifies the complex data from FT-IR spectra into principal components, highlighting variations and patterns that distinguish different species. This combination allows for efficient classification and authentication of herbal materials even when dealing with preprocessed samples (Brangule et al. 2020, Pramod et al. 2011). Overall, FT-IR spectroscopy coupled with PCA is a robust method for the quality verification of herbal raw materials, offering advantages such as non-destructive testing, minimal sample preparation, and high accuracy in species identification. This method addresses the challenges posed by morphological similarities and environmental variations, providing a reliable alternative for manufacturers and quality control laboratories.

MATERIALS AND METHODS

Instruments and apparatus

IR spectra were recorded on a Spectrum 100 Fourier-transform infrared (FT-IR) spectrometer (PerkinElmer, CA, USA) equipped with a mid-infrared deuterated triglycine sulfate (DTGS) detector. The spectra were obtained in the frequency range 4000–450 cm^{-1} with a resolution of 4 cm^{-1} and a total accumulation of 16 scans. A portable and programmable temperature controller (4000 series TM High Stability Temperature Controller, Specac, Ltd.) was used in the temperature range of 50–120°C.

Sample collection

The rhizomes of *K. paviflora, C. caesia*, and *C. aeruginosa* were collected and purchased randomly from 23 locations in Peninsular Malaysia. A total of 53 samples consisted of 19 samples of *K. paviflora*, 17 sample of *C. caesia* and 17 samples of *C. aeruginosa* were collected from Alor Gajah, Melaka; Machang, Kelantan; Maran, Pahang; MARDI, Jerangau Terengganu; Urban Ecolife Agrofarm, Gombak, Selangor; Banting, Selangor; Floranika, Sg. Buloh, Selangor; Agrofarm Gombak, Selangor; Aryen, Sg. Buloh, Selangor; Daun Hijau Organik, Machang, Kelantan; DNR Rumah Herba Kuala Pilah, N. Sembilan; Nursery Masyitah; Paya Asli Herba Quadri Farm, Kuala Nerang, Kedah; Seri Subuh Agrofarm, Tanjung Ipoh, N. Sembilan; Kasih Herbs Nursery, Perlis; Amansah Ahmad, Felda Jengka 18, Maran, Pahang; Seri Kembangan Selangor; Serdang Selangor; Taman Intan Cempaka, Penang; Bandar Sri Damansara; Kebunurai, Kg Padang Tembak, Perak; Amansah Ahmad, Felda Jengka 18,

Maran, Pahang and Rena Hamdan, Shah Alam, Selangor. The rhizomes of each plant were used for the IR analysis (Figure 1).

FT-IR Procedures and Data preprocessing for second derivative and two-dimensional correlation spectrum

Rhizomes were cut into smaller pieces, oven-dried, and ground into a powder. Briefly, 2 mg of each sample was mixed with 100 mg of potassium bromide (KBr), and the mixture was further ground and pressed into a disc with a diameter of 13 mm. IR spectra were recorded from 16 scans in the range of 4000–450 cm^{-1} with a resolution of 4 cm^{-1}. The second-derivative spectra were obtained using a Savitzky–Golay filter through 13 point smoothing which aimed for minimum distortion by least squares fitting a cubic polynomial. For the acquisition of 2D-IR spectra, each sample disc was placed in a sample pool connected to a temperature controller. Dynamic spectra were collected at different temperatures ranging from 50 °C to 120 °C at intervals of 10 °C. 2D-IR correlation spectra were acquired by treating the series of temperature-dependent dynamic spectra with 2D-IR correlation analysis employing the Softdoc software developed by Tsinghua University (Beijing, China).

Data preprocessing for principal component analysis (PCA) of IR spectra

All infrared (IR) spectra were initially subjected to baseline correction to remove any background noise and improve the accuracy of the spectral data. Following baseline correction, the spectra were normalised using the peak area normalisation method, which involved integrating the area under significant peaks to standardise the spectra for comparative analysis. This step ensured that variations in sample concentration or path length were minimised. The preprocessed spectral data were then analyzed using Principal Component Analysis (PCA), a multivariate statistical technique employed to reduce the dimensionality of the data while preserving the most significant variance. PCA was performed using SIMCA-P software (version 14.1, Umetrics, Umea, Sweden), with unit variance scaling applied to the data matrix before conducting PCA. This scaling method ensured that each variable contributed equally to the analysis by scaling the data to have a mean of zero and a variance of one. In the constructed data matrix, each row corresponded to a sample (observation), and each column represented a wave number (variable), providing detailed information about the chemical composition of the samples.

(a) (b) (c)

Figure 1 Image of rhizomes of (a) *K. parviflora*, (b) *C. caesia* and (c) *C. aeruginosa*

RESULTS AND DISCUSSION

IR spectral analysis

Multi-step infrared spectroscopy, comprising conventional FT-IR, second-derivative infrared spectroscopy, and two-dimensional correlation infrared spectroscopy (2D-IR), was employed to analyze the chemical fingerprints of *Kaempferia paviflora*, *Curcuma caesia*, and *Curcuma aeruginosa*. FT-IR spectroscopy, a rapid and nondestructive method (Lu et al. 2008), detects and quantifies the vibrational bonds between functional groups, revealing the complete chemical characteristics of the samples (Tew et al. 2022).

The 1D FT-IR spectra of the three species (Figure 2) exhibited slight differences in shape and intensity, particularly in the expanded region of 873–1950 cm^{-1}. Peak assignments and their possible compounds are summarized in Table 1. Absorption peaks within the range of 3500–3200 cm^{-1}, corresponding to the O-H stretching vibration, and peaks at 2927–2932 cm^{-1}, related to asymmetric C-H stretching, were observed with similar intensities across all species. Distinct variations in peak positions and intensities were noted in the region of 873–1950 cm^{-1} (Figure 3). The absence of absorption peaks at 1515 cm^{-1}, 1352 cm^{-1}, and 1324 cm^{-1} differentiated C. *caesia* from the other two species. Peaks at 1375 cm^{-1} and 1324 cm^{-1} distinguished *C. aeruginosa*. The unique absorption peak at 1352 cm^{-1}, attributed to the C=C bond commonly found in flavones and isoflavones group of compounds (Krysa et al. 2022), differentiates *K. paviflora*, corroborating its richness in methoxyflavone compounds (Elshamy et al. 2019).

Overall, sixteen absorption peaks were identified, characterising the species (Table 1). Strong peaks appeared at approximately 3200 cm^{-1} (hydroxyl group), 2927–2932 cm^{-1} (saturated hydrocarbons), and 1600 cm^{-1} (aromatic ring skeleton) in all species. Peaks at around 1600 cm^{-1}, 1500 cm^{-1}, 1300 cm^{-1}, and 1200 cm^{-1} are characteristic of flavonoids, representing the skeletal stretching vibrations of aromatic rings A and B and the functional group C-O-C of the C ring. These spectral features support the presence of methoxyflavonol compounds in *K. paviflora* (Elshamy et al. 2019) and curcuminoid compounds in *C. caesia* and *C. aeruginosa* (Ibrahim et al. 2023, Elhawary et al. 2024).

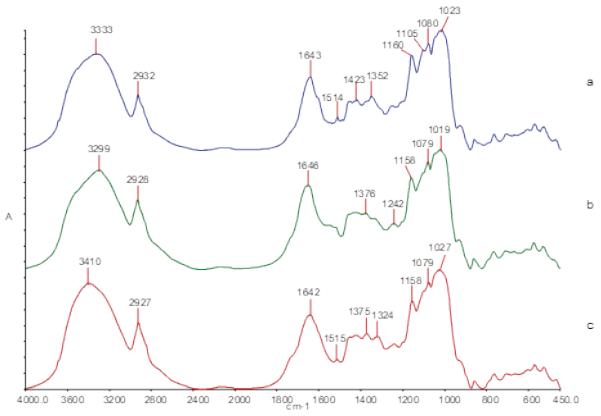

Figure 2 Mean IR spectra of individuals for (a) *K. parviflora*, (b) *C. caesia* and (c) *C. aeruginosa*

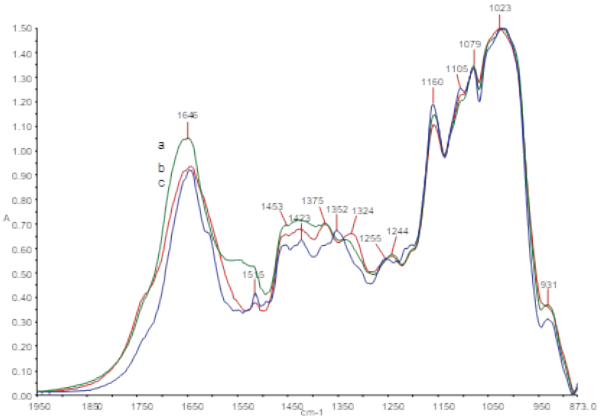

Figure 3 Mean IR spectra of (a) *K. parviflora*, (b) *C. caesia* and (c) *C. aeruginosa* in the expanded region 1950–873 cm^{-1}

Table 1 The preliminary assignment of IR spectra of *C. caesia, C. aeruginosa* and *K. parviflora*

Wavenumber (cm^{-1})	Assignment
3299-3410 (br)	Stretching vibration of bonded and non-bonded –O–H groups
2927-2932 (m)	Asymmetric $–CH_2–$, symmetric $–CH_3$ and $–CH_2–$ stretching vibrations
1642-1646 (s)	=C–H stretching vibration, /amide I/O–H bending vibrations in water
1515 (w)	carbonyl bond vibrations ν(C=O), in plane bending vibrations around aliphatic δ CC-C, δ CC=O and in plane bending vibrations around aromatic δ CC-H of keto and enol configurations and stretching vibrations around aromatic νCC bonds of keto and enolic form
1453 (w)	C–H bending (scissoring) (in CH_3 groups) /aromatic –C=C stretching vibrations
1423 (w), 1375 (w), 1352 (w), 1324 (w)	–OH bending vibrations, –C–O–H in-plane bending vibrations,$–CH_3$ out-of-plane bending vibrations, $–CH_2–$ wagging and twisting vibrations
1255 (w) and 1244 (w)	C(O)–O stretching vibrations and –OH in plane vibrations/ amide III (e.g. in aromatic ethers)
1160 (s)	C–O stretching vibrations (e.g. in C–O–C glycosidic linkages of oligosaccharides or in triacylglycerols)
1105 (w)	Methyl or phenyl
1079 (sh)	C–1–H bending vibration in sugars
1023(sh)	C–4–OH (typical for glucose residue of disaccharides)
931 (w)	trans = C–H out-of-plane bending

Br = broad, s = strong, sh = sharp, m = medium, w = weak

Second derivative spectral analysis

Second-derivative IR spectroscopy is the second step in multi-step IR spectroscopy, which can enhance the spectral resolution by amplifying tiny differences in the IR spectrum (Liu et al. 2006, Huang et al. 2008, Wu et al. 2008). The representative second-derivative spectrum was chosen for each species based on a comparative analysis, as shown in Figure 4. Some of the overlapped absorption peaks can be resolved by second-derivative spectral analysis, which resulted in more dissimilarities, especially in the region of 1800–1300 cm^{-1}. Distinctive strong and sharp absorption peaks at 1605 cm^{-1} and 1492 cm^{-1}, which occurred only in *K. parviflora*, were characteristic features distinguishing *K. parviflora* from the other two species. The latter two species can be further distinguished based on the absence of obvious peaks at 1489 cm^{-1} and 1324 cm^{-1} in *C. caesia*. Thus far, the results suggest that a combination of IR and second-derivative IR spectra can be used to distinguish different samples in terms of closely related species. However, the task of finding discriminating differences among spectra is very demanding and difficult simply by visual examination, especially when dealing with a large number of samples. Therefore, it is more practical to incorporate a statistical method to aid the interpretation of spectroscopic data. Moreover, the discrimination of different varieties of herbs based on slight differences among particular absorption peaks could be subjective, and the results may vary among analysts. Therefore, we subjected the spectroscopic data to chemometric analysis to discriminate the samples more reliably.

Principal component analysis (PCA)

IR spectra are usually wide data matrices characterised by a large number of variables. PCA is a popular method in applied statistical work and data analysis, and it has a good ability to summarize multivariate variations. It allows visualization of the information of the dataset in a few principal components while retaining the maximum possible variability within that set (Chen et al. 2008). The PCA-class is utilised to convert and organise the data depending on specific classes or variables. It provides

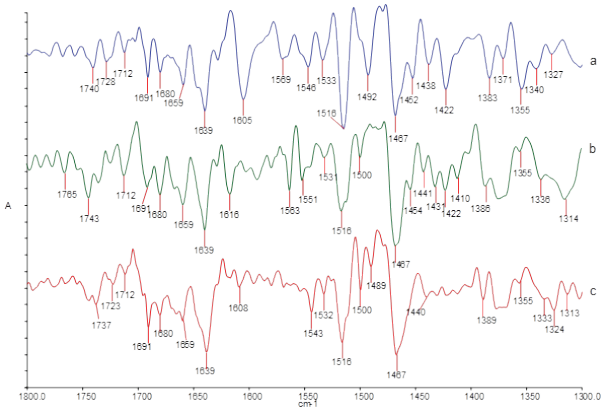

Figure 4 Representative second derivative spectra of (a) *K. parviflora*, (b) *C. caesia* and (c) *C. aeruginosa*

graphical overviews and investigates the general sample distribution trend for outliers, aggregation and dispersion through graphical presentations (Jolliffe & Cadima 2016, Li & Liu 2019). Therefore, PCA is recommended to reduce the computational burden. In this study, preprocessed spectra of *K. paviflora, C. caesia*, and *C. aeruginosa* from different locations were used in the PCA analysis to generate datasets. The data set consisted of 18 spectra of *K. parviflora*, 16 spectra of *C. caesia*, and of 17 spectra. The full region of 1D-IR spectra was used for further analysis, which was defined by 3551 variables corresponding to their wavenumber descriptors. Matrices of 18 × 3351 (*K. parviflora*), 16 × 35551 (*C. caesia*), and 17 × 3351 (*C. aeruginosa*) were constructed, in which the rows are representative of the sample location and species and the columns correspond to the wave number. The results of each analysis are presented as a score plot, which is a map of the samples showing how they are distributed. It can be used to isolate samples that are similar or dissimilar to one another.

Figure 5 depicts a clear separation among samples based on species, as highlighted by the score plot of two principal components (PC1 & PC2). The first two PCs collectively capture an eigenvalue of approximately 99%, with PC1 explaining a variance of 97.3% and PC2, 0.02%. The score plots effectively illustrate the clustering of *K. parviflora, C. caesia,* and *C. aeruginosa* samples from various locations, showcasing PCA's efficacy in grouping samples according to species with noticeable separation between groups. Furthermore, the

inferred variation in raw material composition between species, derived from the cluster space defined by the two PCs, suggests significant differences in chemical composition or other characteristics. This variation implies unique biochemical profiles or distinguishing features for each species, providing valuable insights for botanical, ecological, pharmacological, and environmental studies where understanding the distinct properties and potential uses of these materials is crucial.

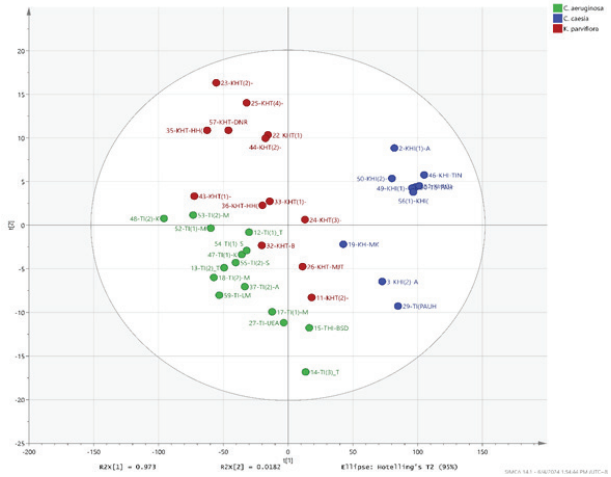

Figure 5 PC scores plots of (a) *K. parviflora*, (b) *C. caesia* and (c) *C. aeruginosa* from various location

Two-dimensional (2D) correlation IR spectral analysis

Two-dimensional (2D) correlation IR spectral analysis involves applying an external perturbation to a sample and measuring a series of IR dynamic spectra, utilising mathematical correlation analysis techniques. The resulting 2D-IR correlation spectra reveal the sensitivity of each IR band or functional group, correlations between different functional groups, and the order of influence during external perturbation. These spectra can enhance spectral resolution, provide dynamic information on molecular structure, and elucidate interactions among functional groups within or between molecules. In synchronous spectra, auto-peaks on the diagonal line indicate the self-correlativity and susceptibility of specific normal vibrations of functional groups to temperature changes. Cross peaks, located off-diagonally, reveal the intensity variations between pairs of group vibrations corresponding to their frequencies. Positive cross peaks signify consistent population changes, either simultaneous increases or decreases, of different groups under external perturbation, with stronger cross peaks indicating more coordinated intensity changes. Representative synchronous auto-peak plots for *K. parviflora*, *C. caesia*, and *C. aeruginosa* in the 1800–1300 cm^{-1} range illustrate distinct auto-peak patterns for each species. *K. parviflora* exhibits nine auto-peaks at 1048 cm^{-1}, 1110 cm^{-1}, 1168 cm^{-1}, 1217 cm^{-1}, 1239 cm^{-1}, 1367 cm^{-1}, 1380 cm^{-1}, 1508 cm^{-1}, and 1660 cm^{-1}. *C. caesia* displays ten auto-peaks, including peaks at 1020 cm^{-1}, 1050 cm^{-1}, 1076 cm^{-1}, 1168 cm^{-1}, 1239 cm^{-1}, 1331 cm-1, 1369 cm^{-1}, 1436 cm^{-1}, 1609 cm^{-1}, and 1651 cm^{-1}, with a unique peak at 1609 cm^{-1} corresponding to carbonyl vibration. *C. aeruginosa* shows nine auto-peaks at 1050 cm^{-1}, 1076 cm^{-1}, 1110 cm^{-1}, 1168 cm^{-1}, 1267 cm^{-1}, 1329 cm^{-1}, 1371 cm^{-1}, 1468 cm^{-1}, and 1661 cm^{-1}. Despite profile similarities, *C. caesia* uniquely features an auto-peak at 1609 cm^{-1}, corresponding to carbonyl vibration, indicating a higher abundance of carbonyl compounds compared to *C. aeruginosa* and *K. parviflora*. Further analysis of synchronous 2D-IR contour plots (Fig. 6b) unveils strong cross peaks at peak at 1068 cm^{-1}, peak 1138 cm^{-1}, and peak 1229 cm^{-1} in *K. parviflora*, distinguishing it from *C. caesia* and *C. aeruginosa*. Both *C. caesia* and *C. aeruginosa* exhibit evident cross peaks at 1600 cm^{-1} and 1640 cm^{-1}, with an additional cross peak at peak 9 in *C. caesia* spectra, amplifying the differences between *C. caesia* and *C. aeruginosa*. Analysis of synchronous 2D-IR contour plots further distinguishes the species, with *K. parviflora* showing strong cross peaks at specific peaks, and *C. caesia* and *C. aeruginosa* displaying additional distinct cross peaks, highlighting their differences.

CONCLUSION

The results showed that IR spectra exhibited variations for the different species but more apparent features were observed in their second derivative spectra which were able to discriminate the raw materials of different species. It is known that the spectral differences

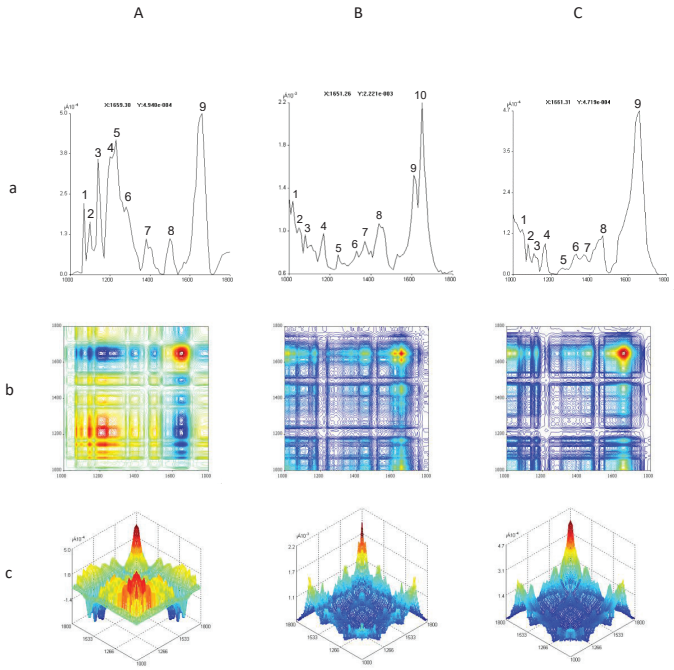

Figure 6 (a) Synchronous 2D-IR auto-peaks plots in the range of 1800–1000 cm^{-1} (b) Synchronous 2D-IR contour plots in the range of 1900–1000 cm^{-1} (c). 1Synchronous 2D-IR mesh plots in the range of 1900–1000 cm^{-1} and (c), for *K. parviflora* (A), C. *caesia* (B) and *C. aeruginosa* (C)

are the objective reflections of the different chemical constituents in tested samples. Analysis and comparison of the IR spectra showed that different origins of the materials gave rise to different chemical constituents. IR spectroscopy combined with chemometric analysis is a useful tool for identifying and differentiating these three species. The 2D-correlation analysis provided additional information on the similarities and dissimilarities under thermal perturbation. This study provides useful information on nondestructive analysis as an alternative approach for the quality control of herbal materials. The results provide a new and rapid operational procedure as well as characteristic data for identification purposes. However, for their genuine and unambiguous identification, morphological identification approach should precede this technique.

ACKNOWLEDGEMENTS

Authors would like to thank the staff of Ethnobotanical Garden, Forest Research Institute Malaysia for their technical assistance in sample collections.

REFERENCES

Brangule A, Šukele R & Bandere D. 2020. Herbal Medicine Characterization Perspectives Using Advanced FTIR Sample Techniques – Diffuse Reflectance (DRIFT) and Photoacoustic Spectroscopy (PAS). *Frontiers in Plant Science*. Vol 11.

Brereton RG. 2003. *Chemometrics, Data Analysis for the Laboratory and Chemical Plant*. John Wiley & Son Ltd., England.

Chen Y, Zhu SB, Xie MY et al. 2008. Quality control and original discrimination of *Ganoderma lucidum* based on High-Performance Liquid Chromatographic fingerprints and combined chemometrics methods. *Analytica Chimica Acta* 623: 146–156.

Elhawary EA, Moussa AY & Singab Anb. 2024. Genus Curcuma: Chemical and ethnopharmacological role in aging process. *BMC Complementary Medicine and Therapies*. 24: 31.

Elshamy AI, Mohamed TA, Essa AF et al. 2019. Recent advances in *Kaempferia*: Phytochemistry and biological activity: A comprehensive review. *Nutrients*, 11: 2396.

Fauziah A, Ling SK, Salbiah M et al. 2012. Characterization and identification of Labisia pumila by Multi-steps Infrared spectroscopy. *Vibrational Spectroscopy* 62: 200–206

Huang A, Zhou Q, Liu J, Fei B, & Sun S. 2008. Distinction of three wood species by Fourier Transform Infrared spectroscopy and Two-dimensional Correlation IR spectroscopy. *Journal of Molecular Structure*. 883:160–166.

Ibrahim H, Khalid N & Hussin K. 2007. Cultivated gingers of Peninsular Malaysia: Utilization, profiles and micropropagation. *Gardens' Bulletin Singapore* 59: 71–88.

Ibrahim Nna, Wan Mustapha Wa, Sofian-Seng Ns et al. 2023. Comprehensive review with future prospects on the medicinal properties and biological activities of *Curcuma caesia* Roxb. *Evidence-Based Complementary and Alternative Medicine*. Vol. 2023. https://doi.org/10.1155/2023/7006565.

Liu Hx, Sun Sq, Lv GH & Chan KK. 2006. Study on Angelica and its different extracts by Fourier Transform Infrared spectroscopy and Two-dimensional Correlation IR spectroscopy. *Spectrochimica Acta Part A*: *Molecular and Biomolecular Spectroscopy*. 64: 321–326.

Liu Hx, Zhou Q, Sun Sq & Bao HJ. 2008. Discrimination of different *Chrysanthemums* with Fourier Transform Infrared spectroscopy. *Journal of Molecular Structure*. 883: 38–47.

Lu GH, Zhou Q, Sun SQ et al. 2008. Differentiation of Asian ginseng, American ginseng and *Notoginseng* by Fourier Transform Infrared spectroscopy combined with Two-dimensional Correlation Infrared spectroscopy. *Journal of Molecular Structure*. 883-884: 91–98.

Leong–Skornickova J, Sida O & Marhold K. 2010. Back to types! Towards stability of names in Indian *Curcuma* L. (Zingiberaceae). *Taxon*. 59: 269–282.

Martyna K, Monika SC & Artur Z. 2022. FT-IR and FT-Raman fingerprints of flavonoids: A Review. *Food Chemistry*. Vol. 393. 133430, ISSN 0308-8146.

Nik Musa'adah M, Nik Zanariah Nm, Nor Azah Ma & Norini H. (eds.) 2017a. Khazanah Perubatan Melayu: Tumbuhan Ubatan Jilid 1. Institut Penyelidikan Perhutanan Malaysia, Kepong, Selangor.

Bik Musa'adah M, Nik Zanariah NM, Nor Azah MA & Norini H. (eds.) 2017b. Khazanah Perubatan Melayu: Tumbuhan Ubatan Jilid 2. Institut Penyelidikan Perhutanan Malaysia, Kepong, Selangor.

Noda I. 1993. Generalized two-dimensional correlation method applicable to Infrared, Raman, and other types of spectroscopy. *Applied Spectroscopy* 47: 1329–1336.

Noda I, Dowrey AE, Marcott C et al. 2000. Generalized two-dimensional correlation spectroscopy. Applied Spectroscopy. 54: 236A–248A.

Pramod S, Harish CA, Rawat Msm et al.2011. Fourier Transform Infrared (FT-IR) spectroscopy in An-Overview. *Research Journal of Medicinal Plants*, 5: 127–135.

Ridley HN. 1924. The Flora of the Malay Peninsula. Volume IV. L. Reeve & Co. Ltd., London.

Sadegh KA, Javad F, Fatemeh M & Maryam F. 2016 Detection and quantification of food colorant adulteration in 2 saffron sample using chemometric analysis of FT-IR spectra. *RSC Adv.*, 10.1039. C5RA25983E–. doi:10.1039/C5RA25983E.

Tan HP, Ling SK & Chuah CH. 2010. Multi-step Infrared macro-fingerprinting on leaves of *Phyllagathis praetermissa* from different localities in Peninsular Malaysia. *Vibrational Spectroscopy*. 52: 48–53.

Tew WY, Ying C, Wujun Z et al. 2022. Application of FT-IR spectroscopy and chemometric technique for the identification of three different parts of *Camellia nitidissima* and discrimination of its authenticated product. *Frontiers in Pharmacology*. Vol. 13.

Than TY & Kyi Wyl. 2019. Study of phytochemical composition on *Kaempferia parviflora* Wall. ex Baker. IEEE–SEM 7: 128–136.

Wu YW, Sun SQ, Zhao J, LI Y & Zhou Q. 2008. Rapid discrimination of extracts of Chinese propolis and poplar buds by FT-IR and 2D IR correlation spectroscopy. *Journal of Molecular Structure*. 883: 48–54.